VRF — nuclear spectral analysis with non-linear full-spectrum nuclide shape fitting

George Lasche[1,*], *Robert* Coldwell[2], and *Robert* Metzger[3]

[1]Snakedance Scientific, LLC, 13509 Quaking Aspen Place NE, Albuquerque, NM 87111, USA
[2]Coldwell Consulting, 1520 NW 40th Drive, Gainesville, FL 32605, USA
[3]Radiation Safety Engineering, Inc, 3245 North Washington Street, Chandler, AZ 85225, USA

Abstract. A new application (known as “VRF”, or "Visual RobFit") for analysis of high-resolution gamma-ray spectra has been developed using non-linear fitting techniques to fit full-spectrum nuclide shapes. In contrast to conventional methods based on the results of an initial peak-search, the VRF analysis method forms, at each of many automated iterations, a spectrum-wide shape for each nuclide and, also at each iteration, it adjusts the activities of each nuclide, as well as user-enabled parameters of energy calibration, attenuation by up to three intervening or self-absorbing materials, peak width as a function of energy, full-energy peak efficiency, and coincidence summing until no better fit to the data can be obtained. This approach, which employs a new and significantly advanced underlying fitting engine especially adapted to nuclear spectra, allows identification of minor peaks that are masked by larger, overlapping peaks that would not otherwise be possible. The application and method are briefly described and two examples are presented.

1 Introduction

Applications for nuclear spectral analysis that are now in wide use for commercial applications typically begin with a peak search (such as the Mariscotti [1] method of second derivatives), and then match the energies and areas of the peaks that were found to nuclear tables to determine the activities of nuclides evident in the spectrum, taking into account calibrations for energy, resolution (or "peak-width"), and detector efficiency. This approach has difficulty resolving peaks that lie closely together unless they are sufficiently well separated in energy, have comparable areas, and have sufficient counting statistics.

These limitations can be overcome with a different approach using minimization of the chi-squared statistic, as with the method of Marquardt [2] and detailed in Bevington [3], of full-spectrum shapes for all the nuclides under consideration. This requires, however, that the second derivative matrix can be successfully inverted, which is often not possible with standard techniques such as described by Press et al. [4] due to the limitations of the numerical precision, computer memory, and processor speed. An extension of the method of Marquardt, known as RobFit [5], has been developed and is capable of inverting large, sparse matrices successfully and rapidly enough to meet the requirements of sophisticated nuclear spectral analysis. An early attempt at applying less-developed versions of RobFit was described by Lasche [6], but the graphical implementation lacked many essential capabilities for practical analysis, the library was severely limited, and the interface that applied nuclear spectral data to RobFit had only limited capabilities for calibration, no gamma emission line search capability, crude efficiency fitting methods, inefficient continuum fitting methods, and no means of identifying or resolving coincidence summing peaks. All of these limitations have been overcome with an entirely new implementation of a greatly improved interface to RobFit called "Visual RobFit", or “VRF” for short.

2 Description

In the recent four years the authors have created an entirely new procedural interface to analyze nuclear spectral data with an improved RobFit engine and a completely new and comprehensive graphical user interface. During analysis, full-spectrum shapes of user-selected emitters are generated by referencing a library consisting of every peak of every nuclide listed in the ENSDF [7], all of the elemental thermal neutron capture peaks and elemental x- rays listed in the TORI [8], and the mass absorption data given by Berger et al. [9] for all of the elements up to atomic number 98, as well as some

* Corresponding author: George.Lasche@alum.mit.edu

common charged-particle reactions. Users are able to add to or edit any of the library data. Equilibrium decay chains can be selected to unify all of the emissions of the nuclides in equilibrium -- this feature is useful not only to apply more known physics for better results, but also to expose impacted nuclides not in equilibrium. Any combination of these emitters can be grouped as subject to up to three differing attenuations by intervening matter.

Each analysis step consists of a series of iterations seeking a best fit while varying the activities of each emitter and the user-enabled parameters of energy calibration, resolution calibration, detector full-energy peak efficiency, and attenuation by intervening compounds or mixtures of material. Also, a single parameter can be allowed to vary for the best fit to all random (or "accidental") coincidence peaks in the spectrum, and another single parameter for all of the cascade (or "true") coincidence peaks in the spectrum. When no further improvement can be made, the analysis step terminates. The values of all activities and other fitted parameters are then reported together with their uncertainties (or "errors") which include the effects of covariance with all other variables in the fit.

3 Validation

In a companion paper [10], automated analysis results for ^{226}Ra and ^{228}Ra from 12 soil samples, and from a sample of synthetic soil spiked with radium from a certified standard, are compared to results from well-known commercial software with excellent agreement. In cases of low-level uranium concentrations, the commercial software was unable to give useful results due to peak interferences and low counting statistics, so results of analysis from VRF were compared to concentrations from certified standards or results from alpha spectrometry, again with excellent agreement. These include impacted uranium in a water sample and certified uranium standard in water at only 0.014 Bq/g. Further validation was conducted with samples of standard thoriated soil, also with excellent agreement with the known values of the NIST-traceable source.

4 Example analysis #1 – uranium metal

A good example well-suited to illustrate the capabilities of VRF is the analysis of a spectrum from a small flat piece of uranium. The spectrum was collected without the benefit of a low-background chamber and the analysis was carried out without the benefit of a local background spectrum. The task was to determine if the sample was natural, depleted, or enriched uranium. With VRF the usual subtraction of a background spectrum for *in situ* measurements is neither needed nor desired — instead, the natural background radiation environment that is mixed with the radiation from the sample gives valuable information about the energy and resolution calibrations and the detector efficiency, and is easily deconvoluted from the peaks caused by radiation from the sample of interest. Furthermore, the use of a single spectrum (rather than subtracting a background spectrum as is common practice) avoids the errors associated with background subtraction and preserves Poisson statistics.

Two groups of emitters were simultaneously fitted during the analysis. The first group, for the natural radiation environment, consisted of ^{40}K, the annihilation reaction peak at 511 keV, and fully-aged equilibrium decay chains of ^{232}Th, ^{238}U, and ^{235}U; the second, for the sample, consisted of uranium x-rays and equilibrium decay chains of ^{238}U and ^{235}U aged more than 5 months (to allow significant growth of ^{234}Th) but less than 5500 years (before significant growth of ^{231}Pa). The first group was designated to be self-absorbed by a typical optical depth of 10 cm of typical soil; the second, self-absorbed by uranium metal an estimated 0.5 cm thick. Four parameters of a cubic polynomial for energy calibration were allowed to vary, and four for resolution also. The thickness of the uranium metal was also allowed to vary during the best-fit minimization process. The fits to all of the peaks of each of the emitters in the region of 778-812 keV is shown in Figure 1, and in the region of 186 keV in Figure 2. In these figures the advantage of whole-spectrum nuclide fitting for resolving overlapping peaks becomes clear.

Because the detector efficiency was not well known, a default efficiency typical of HPGe detectors was used and the activities were reported only as relative to each

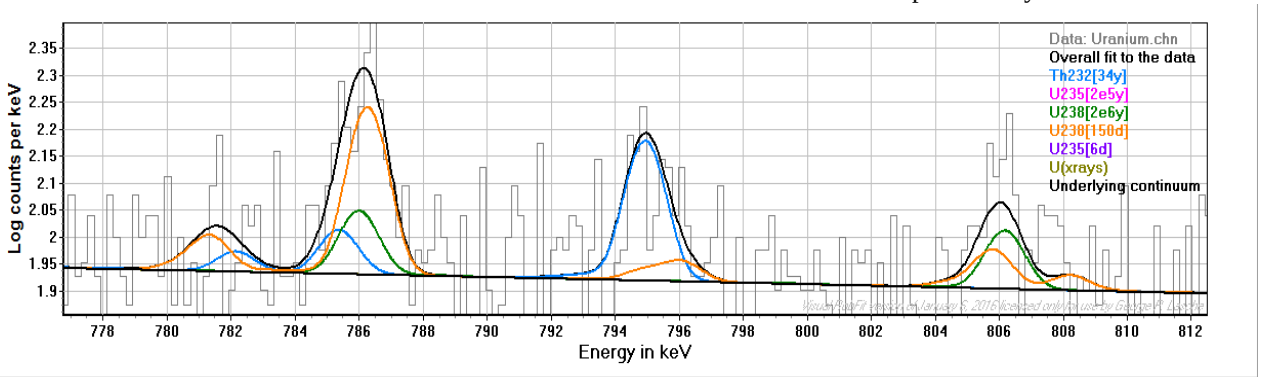

Figure 1. The analyzed spectrum of uranium in the region of 776-811 keV showing the overall fit (black), the fit to recently-processed ^{238}U (orange), the fit to fully-aged ^{232}Th (blue), and the fit to fully-aged ^{238}U (green). Shapes that appear to be skewed are sums of peaks from the same emitter. The 786.27 keV of young ^{238}U appears shifted to higher energy than the 785.96 keV of old ^{238}U at because the peak at 785.96 keV is due to ^{214}Pb, which is only evident in fully-aged ^{238}U due to the long growth times of ^{234}U and ^{230}Th. On the other hand, the peak at 786.27 keV is due to ^{234m}Pa, which is the dominant emitter in ^{238}U that is only recently processed.

other. However, relative activities are sufficient to answer the question of enrichment or depletion. The results of relative activities and their uncertainties for the Figure 3, the calculation of the weight-percent ratio of ^{235}U to (^{235}U + ^{238}U) is shown as 0.2567 +/- 0.0416 percent, with the conclusion that the uranium sample was clearly depleted uranium, which is typically about 0.2% ^{235}U by weight [11], compared to 0.72% for natural uranium, or more for enriched uranium.

5 Example analysis #2 – pipe scale

In this example pipe scale from a new process in a copper mine was found to be radioactive and was sent to us for analysis. Unlike the earlier example of the piece of uranium metal, this spectrum was taken in a low-background chamber and quantitative results were requested.

This example also gives an excellent illustration of the use by VRF of "equilibrium decay chains" in which advantage is taken of the additional physical requirement that all radionuclides in such a chain have fixed activities in relation to each other. VRF considers such chains as if they were single "emitter" whose activity is to be evaluated as if it were a single individual radionuclide.

VRF takes advantage of covariance terms from the matrix inversions that are needed for its non-linear fits. The inclusion of covariance terms, if present, always reduces the statistical uncertainty of the results. VRF uses the ratio of results for activity to the uncertainty of the activity, or "significance", as a measure of confidence that an emitter is present or not. A significance of 5.0 is normally taken as a minimum indication that an emitter is present.

After a quick initial fit of the spectrum it was clear that all the radiation emitters in this spectrum are found in the natural environment. The excessive residuals from an initial fit with the equilibrium decay chains of fully-aged ^{232}Th, ^{238}U, and ^{235}U showed that some of the nuclides were clearly not in equilibrium, so these large decay chains were broken into a continuous sequence of either smaller chains with short equilibration times or individual radionuclides. The next trial assumption was that the longest equilibration time of the smaller chains was 150 days. The test for validity of trial assumptions comes after the analysis by observing if there are no excessive residuals and if the chi-squared statistic of the final fit is satisfactorily low.

Equilibrium decay chains in VRF are labeled with a time to equilibrium in square brackets following the parent nuclide symbol, typically about six half-lives. For example, the fully-aged ^{238}U equilibrium decay chain is represented as U238[2e6y]. For samples such as the pipe second group (the uranium sample) are shown in Figure 3, as well as the fitted thickness of 0.33 cm. Also, in

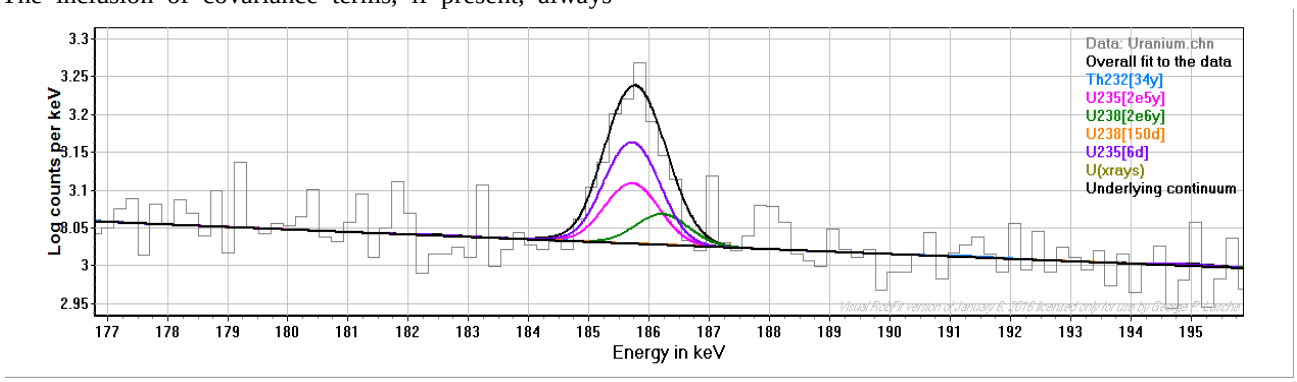

Figure 2. The analyzed spectrum of uranium in the region of 177-195 keV showing the overall fit (black), the fit to recently-processed ^{235}U (purple), the fit to fully-aged ^{235}U (fuchsia), and the fit to fully-aged ^{238}U (green). The peak at 186.2 keV is actually due to ^{226}Ra, a decay daughter of fully-aged ^{238}U. The power of full-spectrum nuclide shape fitting is well-illustrated here. Simple peak-search methods cannot resolve the 186.2 of ^{226}Ra from the 185.7 of ^{235}U, nor can they resolve the 185.7 of ^{235}U due to fully-aged ^{235}U from the 185.7 of recently-processed ^{235}U. Both are critical for determining isotopic ratios of a uranium sample with gamma spectroscopy.

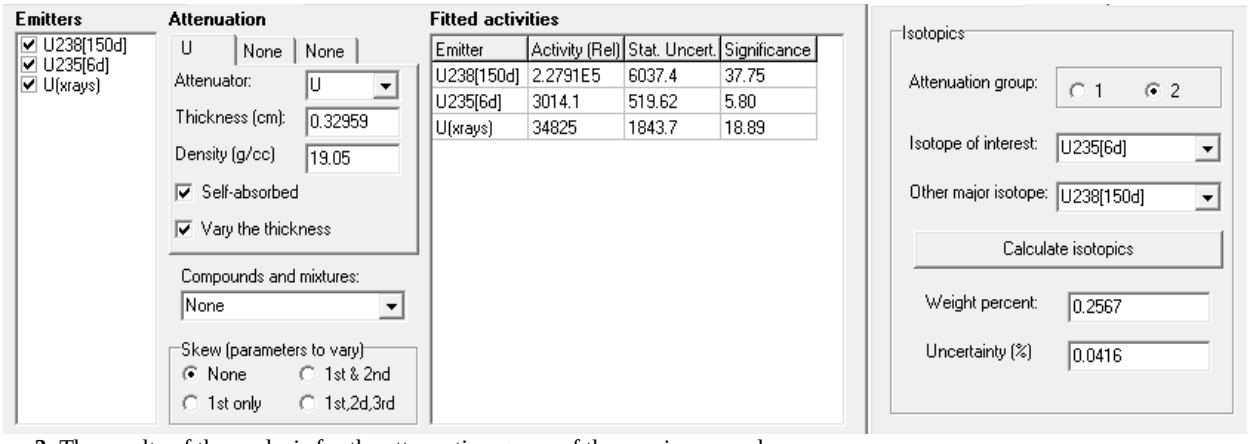

Figure 3. The results of the analysis for the attenuation group of the uranium sample.

scale example, where fully-aged equilibrium clearly cannot be justified for nuclides with very long half lives compared to the age of the sample, VRF provides decay chain segments in which the terminal nuclide of the decay chain segment has a half-life much greater than the half-lives of the other decay daughters of the parent.

The use of decay chain segments is valid if the age of the sample is much greater than the longest half-life of the decay daughters of the parent nuclide of the chain segment, not counting the terminal nuclide.

For example, for processed uranium the ^{238}U decay chain effectively stops at ^{234}U, which has a half-life of 245,490 years. The decay daughter with the longest half-life after the ^{238}U parent and before the ^{234}U terminal nuclide is ^{234}Th, which has a half-life of 24.1 days. If the processed uranium has aged for at least six of the ^{234}Th half-lives, the ^{234}Th and ^{234m}Pa daughters will have essentially the same activity as the ^{238}U parent. However, there is no relation between the activity of the ^{234}U terminal nuclide and the activities of the other members of the chain segment. For the case of processed uranium, VRF represents the decay chain segment for ^{238}U as U238[150d].

For analysis of the pipe scale spectrum, the fully-aged ^{238}U decay chain was broken into four parts:

1. ^{238}U→^{234}Th→^{234m}Pa→^{234}U: This chain segment reaches equilibrium in about 150 days due to the in-growth of ^{234}Th, which has a half-life of 24.1 days. This chain was evident with high significance.

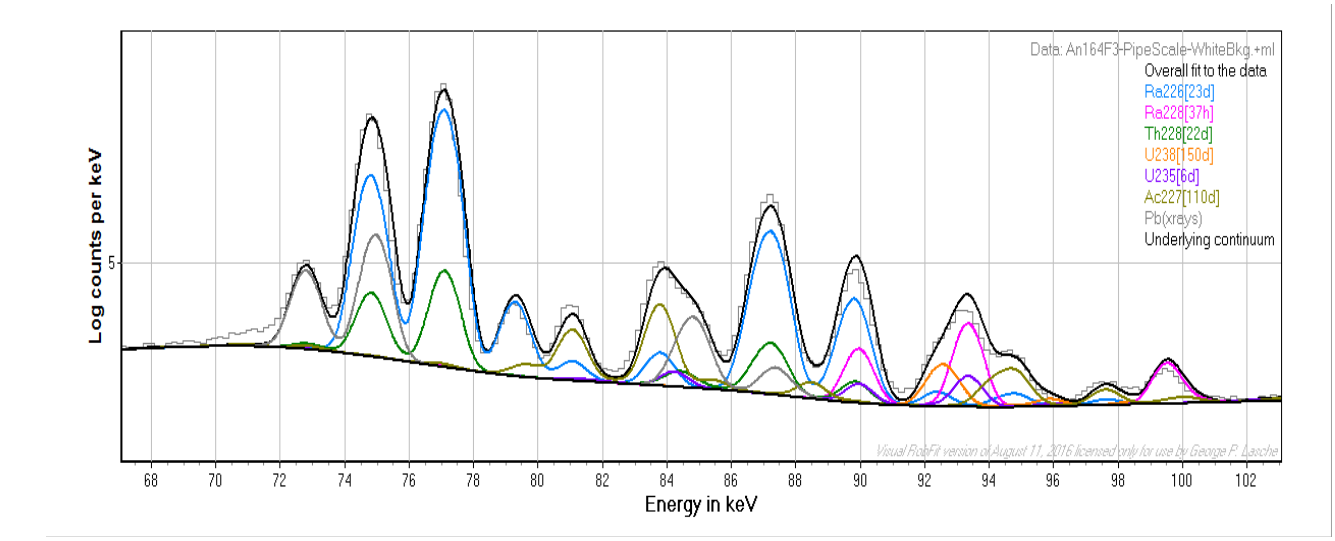

Figure 4. The low-energy region of the spectrum of radioactive pipe scale, as fitted with VRF. Note the deconvolution of the many collided peaks from different emitters in the 92-96 keV region that would not be possible with conventional methods that are based on simple peak-searches.

Table 1. The results from VRF of fitted activities and minimum detectable activities for emitters with low significance. Emitters with text in square brackets in the Emitter column are parent nuclides of an equilibrium decay chain. The equilibration time of the chain is shown in square brackets. The equilibration times of the chains are much less than the half-life of the terminal member of the chain.

Fitted activities

Emitter	Bq/g	Uncertainty	Significance
e+e-	0.016624	0.00091857	18.10
K40	0.08065	0.0072095	11.19
Ra226[23d]	9.2849	0.0063479	1462.68
Ra228[37h]	2.1831	0.0040017	545.55
Th228[22d]	0.81893	0.0019725	415.17
U238[150d]	0.55968	0.01071	52.26
U235[6d]	0.18917	0.0016698	113.29
Th230	0.33051	0.27287	1.21
U234	0.00034723	1.3301	0.00
Ac227[110d]	0.349	0.0015604	223.65
Pb(xrays)	0.49855	0.0025445	195.93
Pa231	0.053006	0.010273	5.16
Th232	1.1852	0.45939	2.58

Fitted minimum detectable activities Group 1

Emitter	Bq/g	Uncertainty	Significance
Th230	1.3201	0.26503	5.0
U234	5.5999	1.1233	5.0
Th232	2.2081	0.44411	5.0

2. ^{234}U: No equilibrium could be assumed due to the long half-life of 245,490 years. It was not detected with minimum significance due to having only low-yield, low-energy gammas, so only its minimum detectable activity (MDA) could be usefully reported.
3. ^{230}Th: No equilibrium could be assumed due to the long half-life of 75,386 years. It was not detected with minimum significance due to having only low-yield, low-energy gammas, so only its minimum detectable activity (MDA) could be usefully reported.
4. ^{226}Ra→^{222}Rn→^{218}Po→^{214}Pb→^{214}Bi→^{210}Po→^{210}Pb→^{210}Bi→^{206}Po→^{206}Pb: This chain segment reaches equilibrium in about 23 days due to the in-growth of ^{222}Rn, which has a half-life of 3.82 days. This chain was evident with very high significance.

The fully-aged ^{235}U decay chain was broken into three parts:

1. ^{235}U→^{231}Th→^{231}Pa: This chain segment reaches equilibrium in about 6 days due to the in-growth of ^{231}Th, which has a half-life of 1.06 days. This chain was evident with high significance.
2. ^{231}Pa: No equilibrium could be assumed due to the long half-life of 32,765 years. This nuclide was evident, however, with minimal significance.
3. ^{227}Ac→^{227}Th→^{223}Ra→^{219}Rn→^{215}Po→^{211}Pb→^{211}Bi→^{207}Tl→^{207}Pb: This chain segment reaches equilibrium in about 110 days due to the in-growth of ^{227}Th, which has a half-life of 18.68 days. This chain was evident with very high significance.

The fully-aged ^{232}Th decay chain was broken into three parts:

1. ^{232}Th: No equilibrium with its ^{228}Ra decay daughter could be assumed because of the evident enhancement of radium in the sample due to an unknown chemical process. It was not detected with minimum significance due to having only low-yield, low-energy gammas, so only its minimum detectable activity (MDA) could be usefully reported.
2. ^{228}Ra→^{228}Ac→^{228}Th: This chain segment reaches equilibrium in about 37 hours due to the in-growth of ^{228}Ac, which has a half-life of 6.15 hours. This chain was evident with very high significance.
3. ^{228}Th→^{224}Ra→^{220}Rn→^{216}Po→^{212}Pb→^{212}Bi→(^{212}Po or ^{208}Tl)→^{208}Pb: This chain segment reaches equilibrium in about 22 days due to the in-growth of ^{224}Ra, which has a half-life of 3.66 days. This chain was evident with very high significance.

With these ten emitters and the addition of emitters for positron annihilation, ^{40}K, and Pb x-rays a satisfactorily low reduced chi-squared of 3.2 was achieved and no excessive residuals were observed, indicating completeness of the analysis. Attempts to achieve a lower chi-squared resulted in what visually appeared to be possible over-fitting, so the analysis was considered complete at that point.

Figure 4 shows the fits to the data in a low-energy region of the spectrum crowded with x-rays and some gammas. Note the deconvolution of the many collided peaks from different emitters in the 92-96 keV region that would not be possible with conventional methods that are based on simple peak-searches.

Table 1 shows the activities of the fitted emitters and the MDA of those with low significance. For each decay chain segment, each member nuclide of the decay chain segment is reported with the same activity, uncertainty, and significance as those of the decay chain segment.

With VRF, MDA is calculated in a different but simple and straightforward manner. The user selects a significance threshold (in this example, a threshold of 5.0 was used). After analysis, MDA is calculated for each emitter that had a significance below the threshold (except for elemental x-ray emitters, thermal neutron capture emitters, and the positron annihilation emitter). For each emitter below threshold VRF adds counts from that emitter's full-spectrum shape to the original spectrum until that emitter can be detected at the desired threshold significance. The resulting activity is the MDA.

6 Conclusion

A new application that uses non-linear fitting of full-spectrum emitter shapes for nuclear spectral analysis has been demonstrated and validated. This application has significant advantages compared to standard peak-search methods, in particular when the resolution of overlapping peaks from different emitters is important.

Emitter shapes can be formed from a single nuclide's gammas and decay x-rays or from an equilibrium decay chain of many nuclides. The non-linear fitting process consists of many automated iterations in which adjustments are made to the activities of each nuclide or decay chain, as well as to user-enabled parameters of energy calibration, attenuation by up to three intervening or self-absorbing materials, peak width as a function of energy, full-energy peak efficiency, and coincidence summing, until no better fit to the data can be obtained.

References

1. M.A. Mariscotti , Nuclear Instrumentation Methods 50 (1967), 309.
2. D.W. Marquardt, Journal of the Society for Industrial and Applied Mathematics, 11 (1963) 431-441.
3. P.R. Bevington, D.K. Robinson, Data Reduction and Error Analysis for the Physical Sciences, McGraw-Hill, New York, 1969, Chapter 11.
4. W.H. Press, S.A. Teukolsky, W.T. Vetterling, B.P. Flannery, Numerical Recipes, Cambridge University Press, New York, 1992, (Sec 15.5).
5. R.L. Coldwell, G.J. Bamford, 1991, The Theory and Operation of Spectral Analysis Using ROBFIT, American Institute of Physics, New York, 1991.

6. G.P. Lasche, R.L. Coldwell, Analysis of Nuclear Spectra with Non-Linear Techniques and its Implementation in the Cambio Application, Journal of Radioanalytical Nuclear Chemistry (2009) 282:211-215.
7. Evaluated Nuclear Structure File (ENSDF), National Nuclear Data Center (NNDC), Brookhaven National Laboratory, www.nndc.bnl.gov/ensdf
8. S.Y.F. Chu, L.P. Ekstrom and R.B. Firestone, WWW Table of Radioactive Isotopes, database version 1999-02-28, http://nucleardata.nuclear.lu.se/nucleardata/toi/
9. M.J. Berger, J.H. Hubbell, S.M. Seltzer, J. Chang, J.S. Coursey, R. Sukumar, and D.S. Zucker, XCOM: Photon Cross Sections Database, National Institute of Standards and Technology, NBSIR 87-3597, 1998.
10. R.L. Metzger, K.A. Van Riper, G.P. Lasche, "Uranium, radium and thorium in soils with high-resolution gamma spectroscopy, MCNP-generated efficiencies, and VRF non-linear full-spectrum nuclide shape fitting", to be published in the proceedings of the ICRS-13 & RPSD-2016, Paris, France, Oct 3-6, 2016.
11. B. Rostker, Properties and Characteristics of DU, U.S. Department of Defense, Dec 13, 2000, http://www.gulflink.osd.mil/du_ii/index.htm#TABC_Properties and Characteristics of DU